JOURNAL OF CHEMICAL INFORMATION AND MODELING

Article

pubs.acs.org/jcim

Neural-Network Scoring Functions Identify Structurally Novel Estrogen-Receptor Ligands

Jacob D. Durrant,[†] Kathryn E. Carlson,[‡] Teresa A. Martin,[‡] Tavina L. Offutt,[†] Christopher G. Mayne,[‡] John A. Katzenellenbogen,[‡] and Rommie E. Amaro*[,†]

[†]Department of Chemistry & Biochemistry and the National Biomedical Computation Resource, University of California, San Diego, La Jolla, California 92093, United States

[‡]Department of Chemistry, University of Illinois at Urbana−Champaign, Urbana, Illinois 61801, United States

Supporting Information

ABSTRACT: The magnitude of the investment required to bring a drug to the market hinders medical progress, requiring hundreds of millions of dollars and years of research and development. Any innovation that improves the efficiency of the drug-discovery process has the potential to accelerate the delivery of new treatments to countless patients in need. "Virtual screening," wherein molecules are first tested in silico in order to prioritize compounds for subsequent experimental testing, is one such innovation. Although the traditional scoring functions used in virtual screens have proven useful, improved accuracy requires novel approaches. In the current work, we use the estrogen receptor to demonstrate that neural networks are adept at identifying structurally novel small molecules that bind to a selected drug target, ultimately allowing experimentalists to test fewer compounds in the earliest stages of lead identification while obtaining higher hit rates. We describe 39 novel estrogen-receptor ligands identified in silico with experimentally determined K_i values ranging from 460 nM to 20 μM, presented here for the first time.

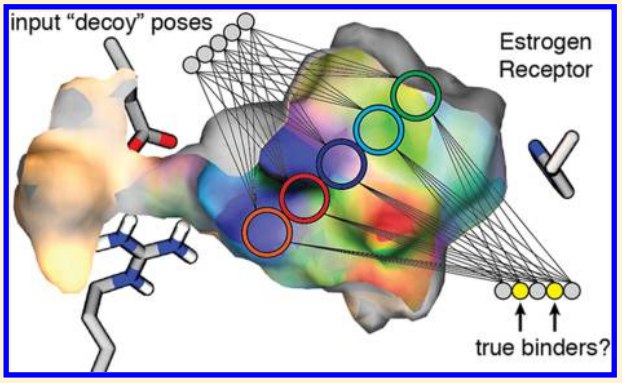

INTRODUCTION

There is an urgent need for innovative approaches to improve the efficiency of the drug-discovery process. The purpose of the current work is to highlight the potential benefits of applying machine learning, specifically neural networks, to structure-based drug discovery. Artificial neural networks (ANN), first conceived in the 1950s,[5] have become popular in recent decades thanks to algorithmic and hardware advances. Although ANN have been applied to drug discovery in the context of ligand-based QSAR (see, for example, ref 6), they have not traditionally been used in structure-based virtual-screening methods. We here confirm that they are well suited to this important task. Given the ever-growing amount of data available for training[7−9] and the recent evolution of GPU-accelerated computation, we believe neural-network-based techniques have the potential to transform the in silico prediction of molecular recognition.

High-throughput biochemical screens are often used to identify pharmacologically active compounds. Although highly automated, these screens require specialized hardware, labor, and carefully managed consumables, making them nontrivial and cost-intensive endeavors that are inaccessible to many researchers in academia and industry. In silico techniques such as virtual screening require only modest computational infrastructure and have become an attractive alternative for lead identification.

Structure-based virtual screening is a two-step process in which a molecule is first docked (i.e., positioned) into a receptor pocket and then evaluated using a scoring function that predicts activity. Reliable scoring functions are required to effectively enrich a set of top-predicted binders with potential hits.[10−16] Great effort has been dedicated to improving their accuracy, although much room for improvement remains.

Durrant et al. recently created two fast and accurate neural-network scoring functions for rescoring docked ligand poses (NNScore 1.0 and 2.0).[17−19] Unlike traditional docking scoring functions, these nonparametric functions are not constrained to predetermined physical formulas or statistical analyses; rather, they "learn" directly from existing experimental data how best to predict binding and so can, in theory, better capture the nonlinear, synergistic relationships among binding determinants. To our knowledge, these are the first neural-network scoring functions that predict affinity by directly examining atomic-resolution ligand−protein interactions.

Machine-learning docking rescoring functions in general, and NNScore in particular, have only recently been described in the

Received: April 27, 2015
Published: August 18, 2015

DOI: 10.1021/acs.jcim.5b00241
J. Chem. Inf. Model. 2015, 55, 1953−1961

literature. Initial studies have shown that this class of scoring functions performs well in *retrospective* studies, as judged by the ability to predict previously determined experimental binding affinities[20] or to separate known ligands from a larger library of presumed nonbinding decoy molecules.[17] However, with some notable exceptions (see, for example, refs 21−23), these kinds of functions have not been extensively used to *prospectively* identify novel ligands, as required for drug discovery.

The purpose of the current work is to provide additional evidence that NNScore is in fact well suited to prospective drug discovery. Building on one of our previous studies,[17] we here use NNScore to identify 39 novel ligands of the estrogen receptor (ER), the target of several drugs used clinically to treat breast cancer,[24,25] osteoporosis,[24] anovulation,[26] dyspareunia,[27] and male hypogonadism.[28]

RESULTS AND DISCUSSION

Background: Neural Networks. The NNScore scoring function is based on artificial neural networks, machine-learning modules that are designed to mimic, albeit inadequately, the microscopic architecture of the brain. Virtual neurons, called neurodes, are connected by virtual axons, called connections. In brief, information to be analyzed is encoded on a set of neurodes called the input layer. This information is processed as it cascades through the neurodes of the network. The final analysis is encoded on a group of neurodes called the output layer. Neural networks are trained by gradually adjusting the connection strengths until the networks can reliably predict the correct output from a given input.

In previous studies, we trained neural networks to predict small-molecule/receptor binding by first generating numeric "descriptors" of thousands of crystallographic binding poses.[18,19] The descriptors used to train NNScore 1.0 included tallies and categorizations of juxtaposed ligand/receptor atoms, summed electrostatic energies, ligand atom types, and rotatable-bonds counts. Training NNScore 2.0 similarly relied on tallies and categorizations of juxtaposed ligand/receptor atoms and summed electrostatic energies, as well as (1) additional molecular interactions/properties as determined by the BINANA algorithm[29] and (2) physics-based terms borrowed from the AutoDock Vina scoring function.[30]

Neural networks were trained to predict the strength of binding from these descriptors by fitting against experimentally measured binding affinities. Specifically, NNScore 1.0 was trained to categorize ligands by potency (high-affinity vs low-affinity binder). In contrast, NNScore 2.0 was trained to predict the binding affinity directly.

Following this training phase, other small-molecule/receptor binding poses to which the networks had never been previously exposed (e.g., from docking studies) could be similarly analyzed. For a given set of binding-pose descriptors, the networks return a score that correlates with the likelihood of high-affinity binding. When a list of docked compounds is ordered by this score, the set of top-ranked molecules is often enriched for true ligands.

In a recent study, we compared the retrospective virtual-screening performance of NNScore 1.0 and 2.0 across ∼40 diverse protein receptors (Figure 1A). This benchmark study suggested that the average performance of NNScore 1.0 is better than that of NNScore 2.0. However, NNScore 2.0 was the superior function for some receptors,[17] highlighting the utility of employing multiple scoring functions in any computer-aided drug-discovery (CADD) project.

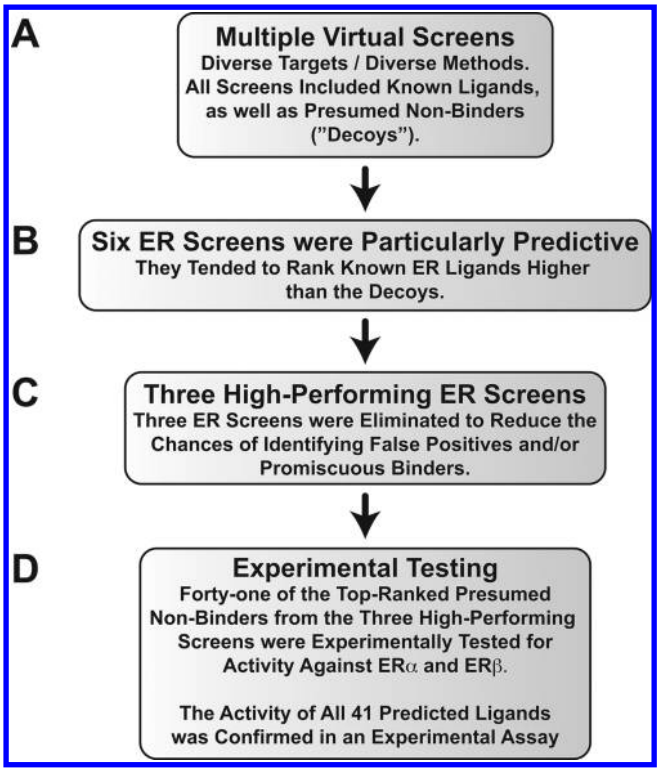

Figure 1. Computational/experimental protocol used to identify novel estrogen-receptor ligands.

Background: NNScore Performance against the Estrogen Receptor. The estrogen receptor alpha (ERα) was among the ∼40 diverse receptors considered previously.[17] Both ERα and the highly homologous ERβ, which differ by only two binding-pocket amino acids[31] (56% sequence identity in the ligand-binding domain[32]), are attractive drug targets.[32,33] These transcription factors are activated by the endogenous steroid hormone 17β-estradiol, leading to gene regulation via binding to specific DNA target sequences. A number of ERα ligands, many of which are nonsteroidal, are currently FDA approved for the treatment of osteoporosis,[24] breast cancer,[24,25] anovulation,[26] dyspareunia,[27] and male hypogonadism.[28] ERβ is emerging as a promising cancer, cardiovascular, inflammatory, and central-nervous-system drug target.[33,34] Various small molecules, including some approved drugs, act as agonists, antagonists, or mixed-function partial agonist/antagonists. The level of agonist vs antagonist activity depends on binding-induced ER-receptor conformational changes,[2,3] as well as on the cellular and even tissue context.[35]

In the previous retrospective virtual-screening study, we used a small-molecule library consisting of known ERα ligands and presumed decoys (e.g., molecules presumed to be nonbinders for testing purposes, though without experimental conformation) taken from the Directory of Useful Decoys (DUD)[36] and the NCI diversity set III (http://dtp.nci.nih.gov/), respectively. The DUD-set ERα agonists and antagonists were docked into their respective ERα structures in the agonist- or antagonist-bound conformations, as appropriate; the same set of NCI decoys was used for both receptors. For each conformation, seven distinct docking/scoring protocols involving AutoDock Vina,[30] Schrödinger's Glide,[37] and NNScore[18,19] were employed.

In six of these virtual screens, over ∼75% of the known ligands were contained in the set of top-ranking compounds

DOI: 10.1021/acs.jcim.5b00241
J. Chem. Inf. Model. 2015, 55, 1953−1961

large enough to include 5% of the presumed decoys (i.e., the true positive rate was >∼75% when the false-positive rate was fixed at 5%, Figures 1B and 2). This metric, which we call the "metric of early performance,"[17] indicates how well a given scoring function is able to enrich the top-ranking compounds with true ligands.

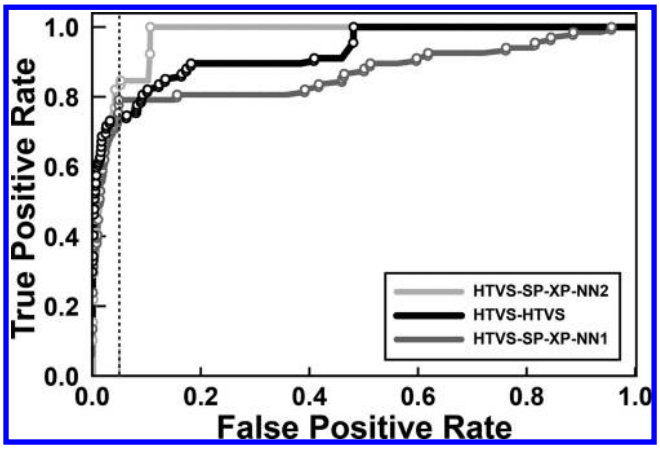

Figure 2. ROC curves associated with each of the three high-performing virtual screens. The data points corresponding to the known ER ligands are shown as circles. The vertical dotted line corresponds to a false positive rate of 5%, used to calculate the early performance metric.

While the vast majority of the top-ranking "decoy" molecules used in the initial study were certainly not true ERα ligands, in the current study we hypothesize that some might in fact be true binders. By showing that this hypothesis is correct, we provide evidence that NNScore can prospectively identify novel ligands from among decoys and therefore has potential for use in structure-based computer-aided drug discovery.

Ignoring Potentially Promiscuous Top-Ranked Compounds. In previous virtual-screening studies, we have noted that certain molecules have a tendency to frequently appear among the top-ranked compounds, even when targeting diverse and unrelated receptors. There are two possible explanations for this phenomenon. First, these compounds may in fact bind to many diverse targets, in which case they are promiscuous and so are poor candidates for drug discovery. Second, they may in fact be nonbinders (false positives) that the scoring functions incorrectly identify as ligands due to inappropriate biases. In either case, such compounds are arguably not worth pursuing.

The six high-performing ERα virtual screens described above identified a number of potentially promiscuous and/or false-positive compounds. Several of the top-ranked compounds were also frequently present among the top-ranked compounds of other high-performing screens from the previously published retrospective study, even though those screens targeted unrelated receptors. To enhance our chances of identifying true and useful ERα ligands, we therefore discarded all virtual "hits" that were found among the top compounds in more than three of the high-performing virtual screens (Figure 1C).

This filtering process had a substantial impact on three of the six high-performing ERα virtual screens. Of the top-ranked compounds from these screens, 14/15 or 15/15 were judged problematic. Given that our goal was to ultimately submit only the top compounds from each screen for experimental testing, we opted to focus exclusively on the other three high-performing ERα screens that were less affected. These screens used the following protocols: (1) compounds were docked with a three-tiered Glide protocol (HTVS/SP/XP) into the ERα *antagonist* conformation and then rescored with NNScore 2.0 (HTVS-SP-XP-NN2/Antagonist); (2) compounds were docked and scored with Glide HTVS into the ERα *agonist* conformation (HTVS/Agonist); and (3) compounds were docked with a three-tiered Glide protocol into the ERα *agonist* conformation and then rescored with NNScore 1.0 (HTVS-SP-XP-NN1/Agonist).

It was fortunate that virtual screens against both the agonist- and antagonist-bound ERα structures performed well. When a small molecule approaches its receptor in vivo, it encounters a flexible binding pocket in constant motion, not a single crystalline conformation.[38] This is especially true of the highly dynamic estrogen-receptor binding pocket, which can assume different geometries depending on the size and shape of the bound ligand.[39,40] Even a scoring function with perfect accuracy could not identify ligands that bind to pockets with unconsidered geometries. By including multiple structurally diverse receptor conformations in virtual-screening campaigns, ligands with a broader diversity of binding poses can potentially be identified.[41]

Evidence for the predictive utility of these three virtual screens was apparent even prior to experimental testing, as two known ERα ligands inadvertently included among the 1560 presumed decoys were correctly identified (genistein, identified by HTVS, and naringenin, identified by both HTVS and HTVS-SP-XP-NN1).

Experimental Confirmation. Forty-one compounds, including genistein and naringenin, were tested experimentally for ERα binding using a competitive radiometric ligand binding assay with an operational sensitivity (limit of detection) of K_i < 20 μM (Figure 1D).[42] Remarkably, all molecules predicted to be ERα ligands in silico had experimental K_i values less than 8 μM. Excluding genistein and naringenin, the most potent novel ERα ligands were NCI-19136, NCI-33005, and NCI-13151, with K_i values of 460, 780, and 1380 nM, respectively (Table 1). Each of these compounds was coincidentally found using a different docking protocol, suggesting that applying multiple CADD techniques to a given target can also increase the diversity of the identified ligands.[43] Though the virtual screens targeted ERα, a similar experimental assay revealed that all 41 compounds bound to ERβ as well (K_i values ≤20 μM). NCI-33005, NCI-13151, and NCI-19136 were notable ERβ binders, with K_i values of 330, 1540, and 2000 nM, respectively (Figure 1D).

These results suggest that (1) NNScore is well suited to prospective drug-discovery projects targeting this system and (2) NNScore can complement more classical scoring functions.

Comparison of Docking Methods. Twenty-nine of the 39 novel ligands presented here for the first time were initially identified using one of the two NNScore protocols, 15 were identified using HTVS, and 3 were identified by both methods. The average K_i values of the compounds found using the HTVS-SP-XP-NN2/Antagonist, HTVS/Agonist, and HTVS-SP-XP-NN1/Agonist protocols were 4.12, 3.68, and 4.10 μM, respectively. A one-way ANOVA analysis led us to reject the null hypothesis that these average K_i values were statistically different (p = 0.76), suggesting that the three protocols performed comparably.

Multiple studies have demonstrated that scoring functions are remarkably receptor specific (see, for example, refs 17 and

DOI: 10.1021/acs.jcim.5b00241
J. Chem. Inf. Model. 2015, 55, 1953−1961

Table 1. High-Affinity Compounds Found by Docking into ERα Structures in Both the Antagonist- and Agonist-Bound Conformations, Sorted by the Experimentally Measured ERα K_i[2,a]

Compound	Structure	ERα K_i (μM)	ERβ K_i (μM)	HTVS-SP-XP-NN2 Percentile	HTVS Percentile	HTVS-SP-XP-NN1 Percentile
NCI-19136 (Figure 4A)	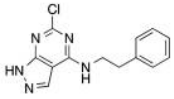	0.46 ± 0.004	2.00 ± 0.4	3.38	(9.47)	(>12.10)
NCI-33005 (Figure 4B)	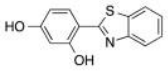	0.78 ± 0.2	0.33 ± 0.1	(5.07)	2.95	(10.88)
NCI-36586 (Genistein)	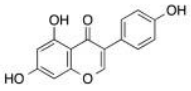	0.79 ± 0.1	0.008 ± 0.00008	(9.69)	2.27	(5.10)
NCI-13151 (Figure 4C)	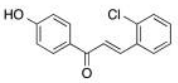	1.38 ± 0.3	1.54 ± 0.3	(>12.50)	(25.88)	2.58
NCI-308849	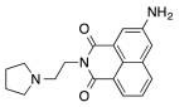	1.38 ± 0.1	4.83 ± 0.1	(>12.50)	(10.76)	2.27
NCI-17128	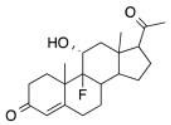	1.81 ± 0.4	4.91 ± 1.4	(>12.50)	(9.40)	3.20
NCI-122253	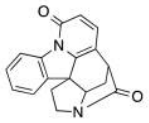	1.98 ± 0.2	5.29 ± 0.9	1.13	1.41	(5.78)
NCI-130847	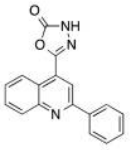	2.05 ± 0.2	6.75 ± 1.5	2.19	(33.74)	(>12.10)
NCI-165701	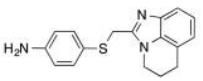	2.47 ± 0	3.16 ± 0.9	(>12.50)	3.38	(5.96)
NCI-34875 (Naringenin)	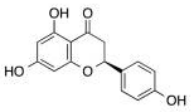	2.56 ± 0.5	3.10 ± 0.9	(4.94)	2.83	3.93
NCI-78623	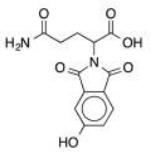	2.78 ± 0.8	3.99 ± 0.6	(11.76)	1.66	(11.25)
NCI-351674	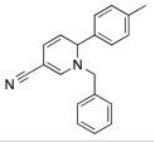	2.82 ± 0.6	8.25 ± 1.4	(5.13)	3.69	(7.68)

DOI: 10.1021/acs.jcim.5b00241
J. Chem. Inf. Model. 2015, 55, 1953−1961

Table 1. continued

Compound	Structure	ERα K_i (μM)	ERβ K_i (μM)	HTVS-SP-XP-NN2 Percentile	HTVS Percentile	HTVS-SP-XP-NN1 Percentile
NCI-12262	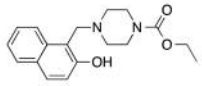	3.08 ± 1.0	11.90 ± 0	(>12.50)	(37.86)	3.44
NCI-201863	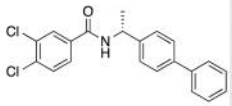	3.18 ± 0.2	7.00 ± 0.4	1.38	(>49.90)	(>12.10)
NCI-95909	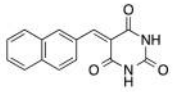	3.74 ± 0.9	7.48 ± 1.4	(>12.50)	(5.10)	1.97
NCI-112541	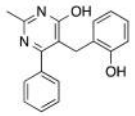	4.14 ± 0.9	5.26 ± 1.3	2.63	(15.49)	(4.79)
NCI-246999	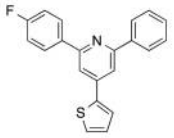	4.32 ± 1.0	3.78 ± 0.1	3.13	(>49.90)	(>12.10)
NCI-319709	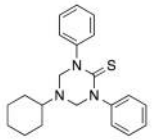	5.20 ± 1.2	6.88 ± 0.7	2.94	(>49.90)	(>12.10)
NCI-117554	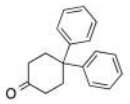	5.25 ± 1.1	7.48 ± 1.4	(5.63)	(5.47)	3.38
NCI-111847	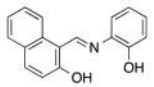	5.42 ± 0.4	7.43 ± 0.5	1.63	(4.12)	3.87

[a]Additional experimentally validated ligands are described in the Supporting Information. Note that the compounds themselves were tested only for binding, not for agonism vs antagonism. For each docking protocol/compound, we report the percentile rank (NCI and DUD compounds considered together). When a given compound did not rank high enough to warrant experimental follow up, the percentile is given in parentheses. Additionally, a lower bound on the percentile is given for compounds that could not be docked/scored at all. Additional compounds are listed in Tables S1, S2, and S3.

44). Similarly, scoring-function performance may be affected by certain chemical features of the small molecules being screened, especially features used to train the scoring functions themselves. One crude way of measuring potential ligand-based biases is to assess the structural diversity of the ligands identified in a given virtual screen. While scoring functions are not typically trained to maximize ligand diversity, functions that identify a set of validated ligands with substantially reduced structural diversity relative to the source library are perhaps suspect.

While hit diversity can be a useful performance metric, we wish to emphasize its limitations. Screens with low hit diversity are not necessary flawed. One might expect a virtual screen to pull out clusters of structurally analogous true ligands. Similarly, screens with high hit diversity are not necessarily free of bias. A scoring function that inappropriately favors compounds with chemical properties that are structure independent (e.g., high molecular weight, high hydrophobicity, etc.) could incorrectly identify false-positive "hits" that are nonetheless structurally diverse. But we do believe that a substantial lack of chemical diversity between compound clusters may in some cases indicate that the associated scoring functions have been over fitted to favor the known, explored, and nonprotectable chemotypes that generally comprise scoring-function training sets. Generally speaking, an ideal virtual screen should identify diverse and unique molecules, in addition to identifying high-affinity compounds.

Compound diversity and uniqueness can be assessed by classifying compounds according to molecular scaffolds (e.g., molecular graphs).[45−49] The NCI Diversity Set III (NCIDSIII),

DOI: 10.1021/acs.jcim.5b00241
J. Chem. Inf. Model. 2015, 55, 1953−1961

Table 2. Chemical-Diversity Analysis Using Molecular Graphs[a]

compound set	N [number]	N_G [molecular graphs]	N_G/N [diversity ratio]	N_s [singleton graphs]	N_s/N [singleton ratio]
NCI Diversity Set III	1560	652	0.42	475	0.31
HTVS-SP-XP-NN2/Antagonist	15	15	1.0	15	1.0
HTVS/Agonist	15	14	0.93	13	0.87
HTVS-SP-XP-NN1/Agonist	15	13	0.87	12	0.80

[a] N = total number of compounds in the library, N_G = number of molecular graphs in the library, N_G/N = diversity ratio, N_s = number of singleton molecular graph scaffolds, N_s/N = singleton ratio.

which contained the structurally diverse presumed decoys used in the retrospective virtual screens, spanned 652 molecular graphs (Table 2). To facilitate subsequent comparison with other compound sets, this count was normalized by the total number of library compounds, giving a unique-framework (diversity) ratio (i.e., structurally distinct $\text{scaffolds}_{\text{count}}$/total number of $\text{compounds}_{\text{count}}$) of 0.42. To put this number into perspective, if each library compound had a unique graph (i.e., optimal diversity), this ratio would be 1.0. In contrast, if all compounds were analogs with the same scaffold (minimal diversity), the ratio would be close to zero.

As a complementary metric, we also measured the uniqueness of the NCI compounds. 475 molecular graphs were associated with a single compound (i.e., singletons, Table 2). A NCIDSIII singleton ratio of 0.31 was calculated by dividing the number of singletons by the total number of compounds.

We next measured the diversity of the three sets of hits identified using the HTVS-SP-XP-NN2/Antagonist, HTVS/Agonist, and HTVS-SP-XP-NN1/Agonist virtual-screening protocols, respectively. The top hits found using these three methods were comparably diverse. The diversity ratios were 1.0, 0.93, and 0.87, respectively (Table 2). Similarly, the singleton ratios were 1.0, 0.87, and 0.80 for the HTVS-SP-XP-NN2/Antagonist, HTVS/Agonist, and HTVS-SP-XP-NN1/Agonist hits, respectively (Table 2). In all cases, the hits were judged to be even more diverse and enriched in singletons than the NCIDSIII compounds generally.

The fact that our top hits were more diverse and unique than the broader NCIDSIII suggests that the docking protocols used do not unduly favor certain molecular scaffolds.

Binding Poses. The BINANA algorithm[29] was used to identify potential receptor−ligand interactions between the crystallographic pose of estradiol (Figure 3), the native ligand, and the docked poses of NCI-19136, NCI-33005, and NCI-13151 (Figure 4), the three highest affinity novel ERα ligands identified. NCI-33005 and NCI-13151 had very similar docked poses, as did NCI-19136 when the 2H-pyrazole tautomer was considered. Like the native ligand estradiol, NCI-19136 and NCI-33005 are predicted to form hydrogen bonds with residue E353. In contrast, the NCI-13151 pose forms a hydrogen bond with the L387 backbone carbonyl oxygen atom, though a simple rotation of the NCI-13151 hydroxyl group would easily permit a hydrogen bond with E353. Like estradiol, all three ligands may also form T-shaped $\pi-\pi$ interactions with F404. NCI-33005 and NCI-13151 may also form hydrogen bonds with R394, just as the estradiol phenyl hydroxyl group does.

In other ways, the three novel ligands have predicted binding poses unlike that of estradiol. For example, NCI-19136 and NCI-33005 may form additional hydrogen bonds with the L346 backbone carbonyl oxygen atom, and NCI-13151 may form a hydrogen bond with L387, as mentioned above. Also, neither of the novel ligands appears to form a hydrogen bond with H524, apparently failing to exploit one of the interactions

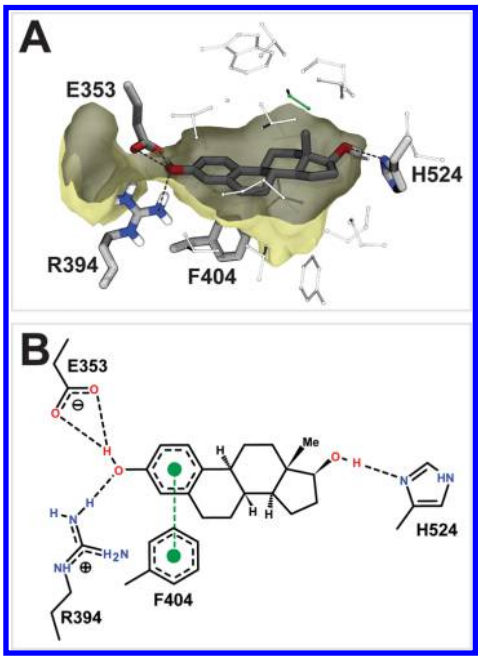

Figure 3. Crystallographic pose of estradiol. (A) The 1G50 crystal structure.[1] (B) Schematic of estradiol binding, modified from output generated by PoseView.[4]

characteristic of estradiol binding. Both ligands do extend aromatic moieties in the direction of H524, however. Modifying these moieties so they can approach and interact with H524 may be an effective drug-optimization strategy, though we do note that a number of other ER ligands (e.g., afimoxifene[2] and raloxifene[50]) have high binding affinities even in the absence of this interaction.

Conclusion. Although the novel scaffolds presented here may be useful for future drug development, ERα has been extensively studied and is already the target of several highly optimized FDA-approved drugs (e.g., tamoxifen, fulvestrant, and raloxifene). The primary utility of the current work is therefore to demonstrate the remarkable performance of two recently developed neural-network docking rescoring functions,[18,19] which, according to a recent retrospective study, are effective against this target as well as a number of others.[17] Herein, we have shown by further computational and experimental analyses that several high-scoring presumed "decoys" indeed bind the receptor target with low micromolar affinity, indicating that these scoring functions are effective when employed prospectively.

Nonparametric machine-learning techniques such as neural networks are often used in ligand-based QSAR, but their application as receptor-centric docking rescoring functions is less common.[18−20,51] These scoring functions take a novel approach to predicting molecular recognition. We believe they

DOI: 10.1021/acs.jcim.5b00241
J. Chem. Inf. Model. 2015, 55, 1953−1961

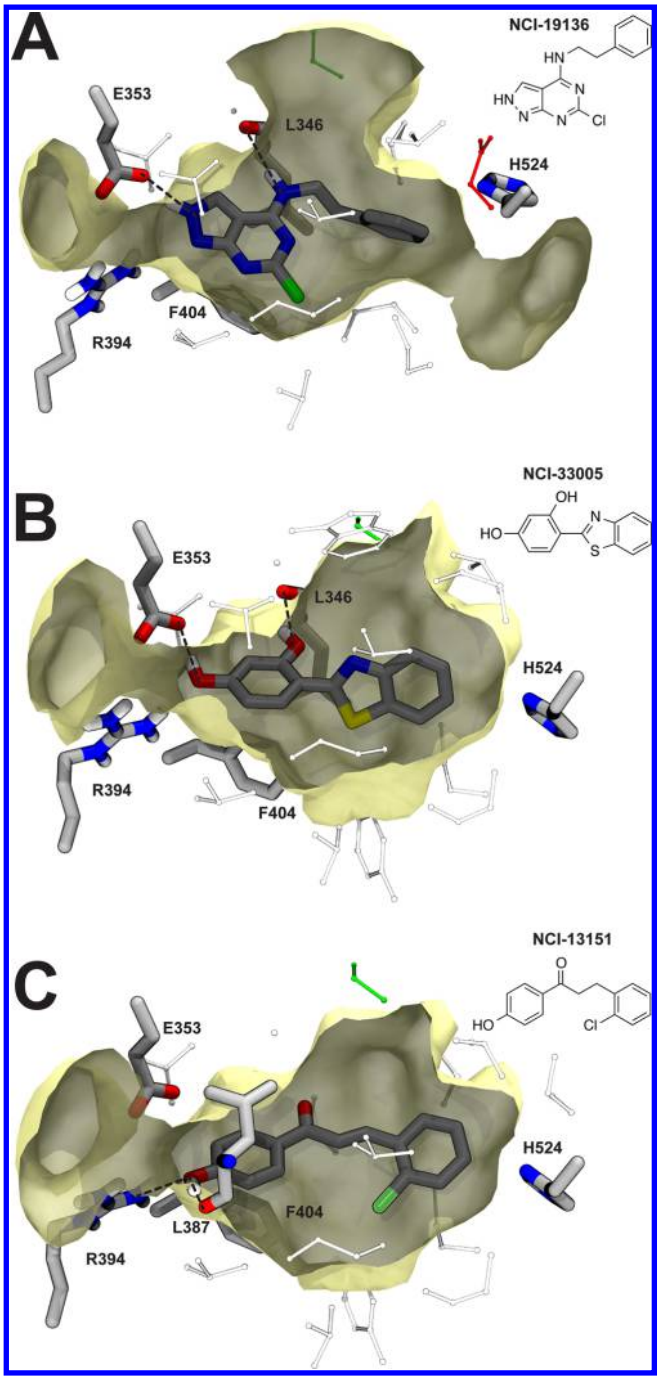

Figure 4. Binding poses. (A) NCI-19136 docked into the 3ERT antagonist structure.[2] Dotted black lines represent hydrogen bonds. (B) NCI-33005, docked into the 1L2I agonist structure.[3] (C) NCI-13151, docked into the 1L2I agonist structure. A potential hydrogen bond with E353 is less certain and so is not shown.

can complement more traditional scoring functions, helping to identify ligand scaffolds that might not be found otherwise.

MATERIALS AND METHODS

Computational Details. Durrant et al. performed a retrospective virtual-screening benchmark study in 2013 to assess the performance of two novel neural-network-based scoring functions, NNScore 1.0 and NNScore 2.0.[17−19] Human estrogen receptor alpha (ERα) in both the agonist- ($ER_{agonist}$) and antagonist-bound ($ER_{antagonist}$) conformations were among the ∼40 diverse receptors considered. In brief, models of $ER_{agonist}$ and $ER_{antagonist}$ were prepared from published crystal structures (PDB IDs 1L2I[3] and 3ERT,[2] respectively). Molecular models of known ERα agonists and antagonists obtained from the Directory of Useful Decoys (DUD)[36] were docked into the relevant receptor, together with 1560 diverse small molecules from the NCI diversity set III (http://dtp.nci.nih.gov/) that served as presumed decoys.

Two high-performing ERα virtual screens targeting $ER_{agonist}$ and $ER_{antagonist}$, respectively, used a multistep docking protocol. Compounds were first docked into each receptor using Schrödinger's Glide HTVS, a fast program designed for high-throughput virtual screening. The compounds were then ranked by the docking score, and the top 50% were subsequently docked using Glide SP, a more computationally demanding program thought to be more accurate. The top 50% of the Glide-SP-docked compounds were then docked using Glide XP, Schrödinger's most rigorous program. Finally, the XP $ER_{agonist}$ and $ER_{antagonist}$ poses were rescored using NNScore 1.0[18] and NNScore 2.0,[19] respectively. These two docking protocols are here called HTVS-SP-XP-NN1/Agonist and HTVS-SP-XP-NN2/Antagonist, respectively. Durrant et al. also obtained an early performance metric[17] of 79% when Glide HTVS alone was used to dock compounds into $ER_{agonist}$ (HTVS/Agonist).

The early performance metric used to assess these three virtual screens was predicated on the assumption that the NCI compounds do not in fact bind to ERα. This assumption is certainly true for the vast majority of these structurally diverse compounds, but it is likely that at least some of the NCI compounds are in fact true ERα ligands. We therefore selected the 15 top-ranked, nonpromiscuous NCI compounds from each of the three high-performing ERα virtual screens for subsequent experimental testing. As some compounds ranked well in multiple screens, forty-one molecules were advanced in total.

Experimental Details. Relative binding affinities were determined by a competitive radiometric binding assay with 2 nM [^{3}H]estradiol as tracer (PerkinElmer, Waltham, MA), as described previously.[52] Full-length purified human ERα and ERβ were purchased from Pan Vera/Invitrogen (Carlsbad, CA). Following incubation for 18−24 h at 0 °C, the receptor−ligand complexes were absorbed onto hydroxyapatite (BioRad, Hercules, CA) and unbound ligand was washed away.[42] All small molecules tested were taken from the NCI Diversity Set III and have purities over 90% per LC/Mass Spec.

Affinities were initially expressed as relative binding affinity (RBA) values, where the RBA of estradiol is set at 100%. Under these conditions, the K_d values of estradiol are ∼0.2 and ∼0.5 nM for ERα and ERβ, respectively. These RBA measurements were reproducible in separate experiments with coefficients of variation of 0.3. The values shown in Table S4 represent the average plus or minus the standard deviation, calculated using two or more independent measurements. The K_i values reported in Table 1 were calculated by dividing the average K_d of estradiol by the RBA and then multiplying by 100.[53]

Chemical Diversity of the Hits. To analyze the chemical diversity and uniqueness of the NCI Diversity Set III, as well as the novel hits identified using the HTVS-SP-XP-NN2/Antagonist, HTVS/Agonist, and HTVS-SP-XP-NN1/Agonist docking protocols, we considered two distinct scaffold representations: Bemis-Murcko frameworks (see the Supporting Information) and molecular graphs (described in the main

DOI: 10.1021/acs.jcim.5b00241
J. Chem. Inf. Model. 2015, 55, 1953−1961

text). Bemis-Murcko frameworks consist of any ring system and linker groups,[48] and molecular graphs consist of nodes (carbon atoms) connected via edges (single bonds). Unlike Bemis-Murcko frameworks, molecular graphs exclude any atom-type or bond-order information. Both the frameworks and graphs were generated using the RDKit package MurckoScaffold.[54]

■ ASSOCIATED CONTENT

Supporting Information

The Supporting Information is available free of charge on the ACS Publications website at DOI: 10.1021/acs.jcim.5b00241.

The Supporting Information lists additional experimentally validated ER ligands beyond those found in Table 1. Further experimental results and analyses of molecular diversity/uniqueness are also provided. (PDF)

■ AUTHOR INFORMATION

Corresponding Author

*E-mail: ramaro@ucsd.edu.

Funding

This work was supported by an NIH Director's New Innovator Award (DP2-OD007237) and an NSF XSEDE Supercomputer resources grant (RAC CHE060073N) to R.E.A., as well as an NIH grant (DK015556) to J.A.K. and an NIH training fellowship (T32ES007326) to T.A.M. Support from the National Biomedical Computation Resource (NBCR, P41 GM103426) is also gratefully acknowledged.

Notes

The authors declare no competing financial interest.

■ ACKNOWLEDGMENTS

We would like to thank Aaron J. Friedman for performing the original Glide virtual screens.

■ ABBREVIATIONS

ER, estrogen receptor; ERα, estrogen receptor alpha; ERβ, estrogen receptor beta; NCIDSIII, National Cancer Institute's Diversity Set III; $ER_{agonist}$, estrogen receptor in the agonist-bound conformation; $ER_{antagonist}$, estrogen receptor in the antagonist-bound conformation; DUD, Directory of Useful Decoys; RBA, relative binding affinity

■ REFERENCES

(1) Eiler, S.; Gangloff, M.; Duclaud, S.; Moras, D.; Ruff, M. Overexpression, Purification, and Crystal Structure of Native Er Alpha Lbd. *Protein Expression Purif.* **2001**, *22*, 165−173.

(2) Shiau, A. K.; Barstad, D.; Loria, P. M.; Cheng, L.; Kushner, P. J.; Agard, D. A.; Greene, G. L. The Structural Basis of Estrogen Receptor/Coactivator Recognition and the Antagonism of This Interaction by Tamoxifen. *Cell* **1998**, *95*, 927−937.

(3) Shiau, A. K.; Barstad, D.; Radek, J. T.; Meyers, M. J.; Nettles, K. W.; Katzenellenbogen, B. S.; Katzenellenbogen, J. A.; Agard, D. A.; Greene, G. L. Structural Characterization of a Subtype-Selective Ligand Reveals a Novel Mode of Estrogen Receptor Antagonism. *Nat. Struct. Biol.* **2002**, *9*, 359−364.

(4) Stierand, K.; Maass, P. C.; Rarey, M. Molecular Complexes at a Glance: Automated Generation of Two-Dimensional Complex Diagrams. *Bioinformatics* **2006**, *22*, 1710−1716.

(5) Rosenblatt, F. The Perceptron - a Probabilistic Model for Information-Storage and Organization in the Brain. *Psychol. Rev.* **1958**, *65*, 386−408.

(6) Agrafiotis, D. K.; Cedeno, W.; Lobanov, V. S. On the Use of Neural Network Ensembles in Qsar and Qspr. *J. Chem. Inf. Model.* **2002**, *42*, 903−911.

(7) Wang, R.; Fang, X.; Lu, Y.; Wang, S. The Pdbbind Database: Collection of Binding Affinities for Protein-Ligand Complexes with Known Three-Dimensional Structures. *J. Med. Chem.* **2004**, *47*, 2977−2980.

(8) Wang, R.; Fang, X.; Lu, Y.; Yang, C. Y.; Wang, S. The Pdbbind Database: Methodologies and Updates. *J. Med. Chem.* **2005**, *48*, 4111−4119.

(9) Hu, L.; Benson, M. L.; Smith, R. D.; Lerner, M. G.; Carlson, H. A. Binding Moad (Mother of All Databases). *Proteins: Struct., Funct., Genet.* **2005**, *60*, 333−340.

(10) Huang, S. Y.; Grinter, S. Z.; Zou, X. Q. Scoring Functions and Their Evaluation Methods for Protein-Ligand Docking: Recent Advances and Future Directions. *Phys. Chem. Chem. Phys.* **2010**, *12*, 12899−12908.

(11) Smith, R. D.; Dunbar, J. B.; Ung, P. M. U.; Esposito, E. X.; Yang, C. Y.; Wang, S. M.; Carlson, H. A. Csar Benchmark Exercise of 2010: Combined Evaluation across All Submitted Scoring Functions. *J. Chem. Inf. Model.* **2011**, *51*, 2115−2131.

(12) Plewczynski, D.; Lazniewski, M.; Augustyniak, R.; Ginalski, K. Can We Trust Docking Results? Evaluation of Seven Commonly Used Programs on Pdbbind Database. *J. Comput. Chem.* **2011**, *32*, 742−755.

(13) Wang, J. C.; Lin, J. H. Scoring Functions for Prediction of Protein-Ligand Interactions. *Curr. Pharm. Des.* **2013**, *19*, 2174−2182.

(14) Cheng, T. J.; Li, Q. L.; Zhou, Z. G.; Wang, Y. L.; Bryant, S. H. Structure-Based Virtual Screening for Drug Discovery: A Problem-Centric Review. *AAPS J.* **2012**, *14*, 133−141.

(15) Yuriev, E.; Agostino, M.; Ramsland, P. A. Challenges and Advances in Computational Docking: 2009 in Review. *J. Mol. Recognit.* **2011**, *24*, 149−164.

(16) Meng, X. Y.; Zhang, H. X.; Mezei, M.; Cui, M. Molecular Docking: A Powerful Approach for Structure-Based Drug Discovery. *Curr. Comput.-Aided Drug Des.* **2011**, *7*, 146−157.

(17) Durrant, J. D.; Friedman, A. J.; Rogers, K. E.; McCammon, J. A. Comparing Neural-Network Scoring Functions and the State of the Art: Applications to Common Library Screening. *J. Chem. Inf. Model.* **2013**, *53*, 1726−1735.

(18) Durrant, J. D.; McCammon, J. A. Nnscore: A Neural-Network-Based Scoring Function for the Characterization of Protein-Ligand Complexes. *J. Chem. Inf. Model.* **2010**, *50*, 1865−1871.

(19) Durrant, J. D.; McCammon, J. A. Nnscore 2.0: A Neural-Network Receptor-Ligand Scoring Function. *J. Chem. Inf. Model.* **2011**, *51*, 2897−2903.

(20) Ballester, P. J.; Mitchell, J. B. O. A Machine Learning Approach to Predicting Protein-Ligand Binding Affinity with Applications to Molecular Docking. *Bioinformatics* **2010**, *26*, 1169−1175.

(21) Lindert, S.; Zhu, W.; Liu, Y. L.; Pang, R.; Oldfield, E.; McCammon, J. A. Farnesyl Diphosphate Synthase Inhibitors from in Silico Screening. *Chem. Biol. Drug Des.* **2013**, *81*, 742−748.

(22) Zhu, W.; Zhang, Y.; Sinko, W.; Hensler, M. E.; Olson, J.; Molohon, K. J.; Lindert, S.; Cao, R.; Li, K.; Wang, K.; Wang, Y.; Liu, Y. L.; Sankovsky, A.; de Oliveira, C. A.; Mitchell, D. A.; Nizet, V.; McCammon, J. A.; Oldfield, E. Antibacterial Drug Leads Targeting Isoprenoid Biosynthesis. *Proc. Natl. Acad. Sci. U. S. A.* **2013**, *110*, 123−128.

(23) Ballester, P. J.; Mangold, M.; Howard, N. I.; Robinson, R. L. M.; Abell, C.; Blumberger, J.; Mitchell, J. B. O. Hierarchical Virtual Screening for the Discovery of New Molecular Scaffolds in Antibacterial Hit Identification. *J. R. Soc., Interface* **2012**, *9*, 3196−3207.

(24) Barrett-Connor, E.; Mosca, L.; Collins, P.; Geiger, M. J.; Grady, D.; Kornitzer, M.; McNabb, M. A.; Wenger, N. K. Effects of Raloxifene on Cardiovascular Events and Breast Cancer in Postmenopausal Women. *N. Engl. J. Med.* **2006**, *355*, 125−137.

(25) Jordan, V. C. Fourteenth Gaddum Memorial Lecture - University of Cambridge - January 1993 - a Current View of

DOI: 10.1021/acs.jcim.5b00241
J. Chem. Inf. Model. 2015, 55, 1953−1961

Tamoxifen for the Treatment and Prevention of Breast Cancer. *Br. J. Pharmacol.* **2000**, *131*, 221−231.
(26) Pfeifer, S.; Fritz, M.; Lobo, R.; McClure, R. D.; Goldberg, J.; Thomas, M.; Pisarska, M.; Widra, E.; Schattman, G.; Licht, M.; Sandlow, J.; Collins, J.; Cedars, M.; Rosen, M.; Vernon, M.; Racowsky, C.; Davis, O.; Dumesic, D.; Odem, R.; Barnhart, K.; Gracia, C.; Catherino, W.; Rebar, R.; La Barbera, A.; Med, A. S. R. Use of Clomiphene Citrate in Infertile Women: A Committee Opinion. *Fertil. Steril.* **2013**, *100*, 341−348.
(27) Unkila, M.; Kari, S.; Yatkin, E.; Lammintausta, R. Vaginal Effects of Ospemifene in the Ovariectomized Rat Preclinical Model of Menopause. *J. Steroid Biochem. Mol. Biol.* **2013**, *138*, 107−115.
(28) Shabsigh, A.; Kang, Y.; Shabsign, R.; Gonzalez, M.; Liberson, G.; Fisch, H.; Goluboff, E. Clomiphene Citrate Effects on Testosterone/Estrogen Ratio in Male Hypogonadism. *J. Sex. Med.* **2005**, *2*, 716−721.
(29) Durrant, J. D.; McCammon, J. A. Binana: A Novel Algorithm for Ligand-Binding Characterization. *J. Mol. Graphics Modell.* **2011**, *29*, 888−893.
(30) Trott, O.; Olson, A. J. Autodock Vina: Improving the Speed and Accuracy of Docking with a New Scoring Function, Efficient Optimization, and Multithreading. *J. Comput. Chem.* **2009**, *31*, 455−461.
(31) Manas, E. S.; Xu, Z. B.; Unwalla, R. J.; Somers, W. S. Understanding the Selectivity of Genistein for Human Estrogen Receptor-Beta Using X-Ray Crystallography and Computational Methods. *Structure* **2004**, *12*, 2197−2207.
(32) Dahlman-Wright, K.; Cavailles, V.; Fuqua, S. A.; Jordan, V. C.; Katzenellenbogen, J. A.; Korach, K. S.; Maggi, A.; Muramatsu, M.; Parker, M. G.; Gustafsson, J. A. International Union of Pharmacology. Lxiv. Estrogen Receptors. *Pharmacol. Rev.* **2006**, *58*, 773−781.
(33) Paterni, I.; Bertini, S.; Granchi, C.; Macchia, M.; Minutolo, F. Estrogen Receptor Ligands: A Patent Review Update. *Expert Opin. Ther. Pat.* **2013**, *23*, 1247−1271.
(34) Minutolo, F.; Macchia, M.; Katzenellenbogen, B. S.; Katzenellenbogen, J. A. Estrogen Receptor Beta Ligands: Recent Advances and Biomedical Applications. *Med. Res. Rev.* **2011**, *31*, 364−442.
(35) Katzenellenbogen, B. S.; Katzenellenbogen, J. A. Biomedicine - Defining the "S" in Serms. *Science* **2002**, *295*, 2380−2381.
(36) Huang, N.; Shoichet, B. K.; Irwin, J. J. Benchmarking Sets for Molecular Docking. *J. Med. Chem.* **2006**, *49*, 6789−6801.
(37) Friesner, R. A.; Banks, J. L.; Murphy, R. B.; Halgren, T. A.; Klicic, J. J.; Mainz, D. T.; Repasky, M. P.; Knoll, E. H.; Shelley, M.; Perry, J. K.; Shaw, D. E.; Francis, P.; Shenkin, P. S. Glide: A New Approach for Rapid, Accurate Docking and Scoring. 1. Method and Assessment of Docking Accuracy. *J. Med. Chem.* **2004**, *47*, 1739−1749.
(38) Gee, A. C.; Katzenellenbogen, J. A. Probing Conformational Changes in the Estrogen Receptor: Evidence for a Partially Unfolded Intermediate Facilitating Ligand Binding and Release. *Mol. Endocrinol.* **2001**, *15*, 421−428.
(39) Katzenellenbogen, J. A. The 2010 Philip S. Portoghese Medicinal Chemistry Lectureship: Addressing the "Core Issue" in the Design of Estrogen Receptor Ligands. *J. Med. Chem.* **2011**, *54*, 5271−5282.
(40) Nettles, K. W.; Bruning, J. B.; Gil, G.; O'Neill, E. E.; Nowak, J.; Hughs, A.; Kim, Y.; DeSombre, E. R.; Dilis, R.; Hanson, R. N.; Joachimiak, A.; Greene, G. L. Structural Plasticity in the Oestrogen Receptor Ligand-Binding Domain. *EMBO Rep.* **2007**, *8*, 563−568.
(41) Durrant, J. D.; McCammon, J. A. Computer-Aided Drug-Discovery Techniques That Account for Receptor Flexibility. *Curr. Opin. Pharmacol.* **2010**, *10*, 770−774.
(42) Carlson, K. E.; Choi, I.; Gee, A.; Katzenellenbogen, B. S.; Katzenellenbogen, J. A. Altered Ligand Binding Properties and Enhanced Stability of a Constitutively Active Estrogen Receptor: Evidence That an Open Pocket Conformation Is Required for Ligand Interaction. *Biochemistry* **1997**, *36*, 14897−14905.
(43) Chen, Z.; Tian, G. H.; Wang, Z.; Jiang, H. L.; Shen, J. S.; Zhu, W. L. Multiple Pharmacophore Models Combined with Molecular Docking: A Reliable Way for Efficiently Identifying Novel Pde4 Inhibitors with High Structural Diversity. *J. Chem. Inf. Model.* **2010**, *50*, 615−625.
(44) Warren, G. L.; Andrews, C. W.; Capelli, A. M.; Clarke, B.; LaLonde, J.; Lambert, M. H.; Lindvall, M.; Nevins, N.; Semus, S. F.; Senger, S.; Tedesco, G.; Wall, I. D.; Woolven, J. M.; Peishoff, C. E.; Head, M. S. A Critical Assessment of Docking Programs and Scoring Functions. *J. Med. Chem.* **2006**, *49*, 5912−5931.
(45) Langdon, S. R.; Blagg, J.; Brown, N. Scaffold Diversity in Medicinal Chemistry Space. In *Scaffold Hopping in Medicinal Chemistry*; Wiley-VCH Verlag GmbH & Co. KGaA, 2013; pp 39−60.
(46) Hu, Y.; Stumpfe, D.; Bajorath, J. Lessons Learned from Molecular Scaffold Analysis. *J. Chem. Inf. Model.* **2011**, *51*, 1742−1753.
(47) Langdon, S. R.; Brown, N.; Blagg, J. Scaffold Diversity of Exemplified Medicinal Chemistry Space. *J. Chem. Inf. Model.* **2011**, *51*, 2174−2185.
(48) Bemis, G. W.; Murcko, M. A. The Properties of Known Drugs 0.1. Molecular Frameworks. *J. Med. Chem.* **1996**, *39*, 2887−2893.
(49) Krier, M.; Bret, G.; Rognan, D. Assessing the Scaffold Diversity of Screening Libraries. *J. Chem. Inf. Model.* **2006**, *46*, 512−524.
(50) Brzozowski, A. M.; Pike, A. C. W.; Dauter, Z.; Hubbard, R. E.; Bonn, T.; Engstrom, O.; Ohman, L.; Greene, G. L.; Gustafsson, J. A.; Carlquist, M. Molecular Basis of Agonism and Antagonism in the Oestrogen Receptor. *Nature* **1997**, *389*, 753−758.
(51) Durrant, J. D.; Amaro, R. E. Machine-Learning Techniques Applied to Antibacterial Drug Discovery. *Chem. Biol. Drug Des.* **2015**, *85*, 14−21.
(52) Katzenellenbogen, J. A.; Johnson, H. J.; Myers, H. N. Photoaffinity Labels for Estrogen Binding Proteins of Rat Uterus. *Biochemistry* **1973**, *12*, 4085−4092.
(53) De Angelis, M.; Stossi, F.; Carlson, K. A.; Katzenellenbogen, B. S.; Katzenellenbogen, J. A. Indazole Estrogens: Highly Selective Ligands for the Estrogen Receptor Beta. *J. Med. Chem.* **2005**, *48*, 1132−1144.
(54) Rdkit: Open-Source Cheminformatics. http://www.rdkit.org/.

DOI: 10.1021/acs.jcim.5b00241
J. Chem. Inf. Model. 2015, 55, 1953−1961